17th World Conference on Earthquake Engineering, 17WCEE
Sendai, Japan - September 13th to 18th 2020

REGULARIZED PLASTIC HINGE MODEL FOR NONLINEAR ANALYSIS OF AXIAL-FLEXURAL RC ELEMENTS

J. Pozo[1], M. Hube[2], Y. Kurama[3]

[1] *Graduate Student, Structural and Geotechnical Engineering, Pontificia Universidad Católica de Chile, and Civil and Environmental Engineering and Earth Sciences, University of Notre Dame, jdpozo@uc.cl*
[2] *Associate Professor, Structural and Geotechnical Engineering, Pontificia Universidad Católica de Chile and Research Center for Integrated Disaster Risk Management CONICYT/FONDAP/15110017, mhube@ing.puc.cl*
[3] *Professor and Associate Chair, Civil and Environmental Engineering and Earth Sciences, University of Notre Dame, ykurama@nd.edu*

Abstract

Distributed plasticity models are commonly used to simulate the nonlinear behavior of axial-flexural reinforced concrete (RC) elements (e.g., slender walls, columns) up to the ultimate displacement at failure. The predicted response from these models is largely governed by the assumed stress-strain constitutive models for the concrete and steel materials. While several traditional models exist for the concrete compressive stress-strain behavior up to crushing, the predicted ultimate (failure) displacement of RC elements when using such constitutive models is highly sensitive to the assumed critical length defined by the integration method (i.e., length where the nonlinear deformations and damage concentrate). Plastic hinge integration methods and material regularization approaches have been separately proposed to obtain an accurate prediction of the ultimate displacement for RC elements with softening post-peak behaviors. However, in the case of plastic hinge integration, the simulated ultimate displacement may be highly sensitive to the assumed plastic hinge length. In the case of regularized material constitutive relationships, the local response of the element (e.g., section curvatures and material strains) may be incorrectly estimated. It may be possible to mitigate these limitations by combining the plastic hinge concept with the material regularization concept. Towards this goal, this paper presents a numerical investigation comparing the cyclic lateral load-displacement simulations of RC walls and columns using plastic hinge models with traditional and regularized concrete and steel stress-strain relationships. Furthermore, a sensitivity analysis of the simulation results to the assumed plastic hinge length is conducted. The study shows that regularized plastic hinge models are capable of accurately simulating the global lateral load-displacement response (including the ultimate displacement) of RC walls, while being mesh insensitive. However, the regularization equations need further improvement for the accurate simulation of ultimate displacement for RC columns.

Keywords: Plastic hinge; material regularization; cyclic behavior; walls; columns.

1. Introduction

Since the use of nonlinear numerical models is becoming common in earthquake engineering design practice, it is essential to develop effective modeling techniques that can accurately predict the behavior of reinforced concrete (RC) elements through failure (e.g., peak strength, ultimate displacement). Previous research towards these modeling goals has focused on lumped plasticity models using semi-empirical equations to define the moment-rotation backbone parameters to simulate RC columns [1,2], and on distributed plasticity models to simulate RC flexural walls [3,4].

Although lumped plasticity models are numerically robust and simple to implement, they present major drawbacks: 1) variations in axial and shear loads cannot be accounted for during the analysis; and 2) there is no standardized guidance for the cyclic moment-rotation relationships [5]. In comparison, distributed plasticity models with fiber sections can allow for more accurate simulations of RC elements because they can capture the variation of axial load in the axial-flexural interaction, and the cyclic response of the element is simulated through cyclic uniaxial concrete and steel material constitutive stress-strain relationships.

It is well known that in distributed plasticity models, the ultimate displacement (i.e., failure displacement) of a RC element with softening post-peak behavior (e.g., due to concrete crushing or rebar buckling) is highly sensitive to the length of the critical integration point over which the nonlinear behavior and failure of the element are concentrated [3,4,6,7]. To reduce this variability, researchers have proposed two approaches: 1) plastic hinge integration methods, in which the length of the critical integration point is matched to an assumed or experimentally-calibrated plastic hinge length [6], and 2) regularized constitutive stress-strain relationships for concrete and steel based on experimentally-calibrated values of post-yield failure energy [4,7]. Each of these approaches has limitations. In the case of plastic hinge integration, the simulated ultimate displacement of the element may be highly sensitive to the plastic hinge length, while in the case of regularized material constitutive relationships, the local response of the element (e.g., section curvatures and material strains) may be incorrectly estimated [4,7]. It may be possible to mitigate these limitations by combining the plastic hinge concept with the material regularization concept. Towards this goal, this paper compares the cyclic lateral load-displacement simulations of RC walls and columns using plastic hinge models with: 1) traditional material stress-strain relationships – defined as "un-regularized plastic hinge models;" and 2) regularized material stress-strain relationships – defined as "regularized plastic hinge models." A sensitivity analysis of the simulation results to the assumed plastic hinge length is also presented.

2. Model Description

The force-based (FB) beam-column element in OpenSees [8] was used to model RC walls and columns in this study. This is a two-node line-element where fiber sections are assigned at integration points (IP) along the length of the element, and plane section deformations are assumed at each IP. Each fiber section is divided into a number of concrete and steel fibers, where nonlinear concrete and steel uniaxial stress-strain material relationships are assigned.

In order to ensure that the length of the critical IP exactly matched the desired plastic hinge length, the FB beam-column element with the modified Gauss-Radau integration method [9] with six integration points was used in both the regularized and un-regularized plastic hinge models. IP locations (x) and integration weights (w) for the modified Gauss-Radau method are presented in Eq. (1), where, L is the total length of the element, L_{pI} and L_{pJ} are the plastic hinge lengths at the two ends, and $L_{int} = L - 4L_{pI} - 4L_{pJ}$. The modified Gauss-Radau method includes integration points at the element ends (i.e., x_1 and x_6 in Eq. (1)), thus accurately modeling the maximum moment at the base of a wall or column element, and integrates quadratic polynomials exactly to provide the exact solution for linear curvature distributions [6].

$$\begin{aligned} x &= \{\ 0;\quad 8L_{pI}/3;\quad 4L_{PI} + L_{int}\left(3-\sqrt{3}\right)/6;\quad 4L_{PI} + L_{int}\left(3+\sqrt{3}\right)/6;\quad L - 8L_{pJ}/3;\quad L\} \\ w &= \{L_{pI};\quad 3L_{pI};\quad 0.5L_{int};\quad 0.5L_{int};\quad 3L_{pJ};\quad L_{pJ}\} \end{aligned} \tag{1}$$

Unconfined and confined concrete fibers were simulated with the *Concrete02* material in OpenSees. The pre-peak compressive stress-strain relationship in *Concrete02* is defined by the Hognestad parabola, with initial stiffness (i.e., Young's modulus) $E_c = 4700\sqrt{f_c'}$ (in MPa units) according to ACI 318-19 [10]. Beyond the peak stress point, which is assumed to be reached at a strain of $\varepsilon_o = 2f_c'/E_c$ for unconfined concrete and $\varepsilon_{co} = 2f_{cc}'/E_c$ for confined concrete (which uses the confined strength ratio, $K = f_{cc}'/f_c'$ according to Mander et al. [11]), the stress-strain relationship reduces linearly to a residual compressive stress. The tensile behavior of the concrete is bilinear, reducing to zero residual stress through tension-softening after cracking. Steel reinforcement was simulated using the Menegotto and Pinto [12] model, which is available in OpenSees as the *Steel02* material. The *MinMax* material model was used in combination with *Steel02* to simulate complete loss of steel compressive stress, representative of buckling, when the ultimate strain of confined concrete, ε_{cu} is exceeded [4]. More details on the un-regularized and regularized materials used in the models are presented next.

The shear force-deformation relationship was incorporated at the section level and was assumed linear-elastic with an effective shear modulus of $G_{eff} = 0.04E_c$ as recommended elsewhere [4,13].

2.1 Un-regularized materials

The ultimate strain of the unconfined concrete was taken as ε_u= 0.004 at a residual stress of $0.2f_c'$, while the ultimate strain of the confined concrete was calculated using Eq. (2) [14], where, ρ_s is the total volumetric ratio of confining steel and ε_{su} is the confining steel strain at maximum tensile stress, which was taken as 0.09.

$$\varepsilon_{cu} = 0.004 + 1.4\rho_s f_y \varepsilon_{su}/f_{cc}' \tag{2}$$

The stress at ultimate strain of confined concrete was obtained following Mander et al. [11] (which uses Popovic's equation), and the *MinMax* material model in OpenSees was used in combination with *Concrete02* to simulate the complete loss of concrete compressive stress upon hoop fracture at ε_{cu}.

2.2 Regularized materials

The concrete and reinforcing steel regularization approaches recommended by NIST [5] for the numerical modeling of slender RC walls were adopted in this study, as conceptually presented in Fig. 1. The regularized ultimate strain for unconfined concrete, ε_u, at residual stress, $R_c f_c'$, was calculated using Eq. (3) and an assumed value of concrete crushing energy, Gf_c. This equation was derived by equating the shaded area of Fig. 1a to Gf_c/L_{cr}, and implies that a larger value of ε_u is required in a model with a smaller critical integration length, L_{cr}. A similar relationship for the ultimate strain of confined concrete, ε_{cu}, can be obtained by replacing the appropriate terms, as shown in Eq. (4).

$$\varepsilon_u = \frac{1}{1+R_c} \cdot \left[\frac{2Gf_c}{f_c' L_{cr}} - \frac{f_c'}{E_c} + (1+R_c)\varepsilon_o + R_c^2 \frac{f_c'}{E_c}\right] \tag{3}$$

$$\varepsilon_{cu} = \frac{1}{1+R_{cc}} \cdot \left[\frac{2Gf_{cc}}{f_{cc}' L_{cr}} - \frac{f_{cc}'}{E_c} + (1+R_{cc})\varepsilon_{co} + R_{cc}^2 \frac{f_{cc}'}{E_c}\right] \tag{4}$$

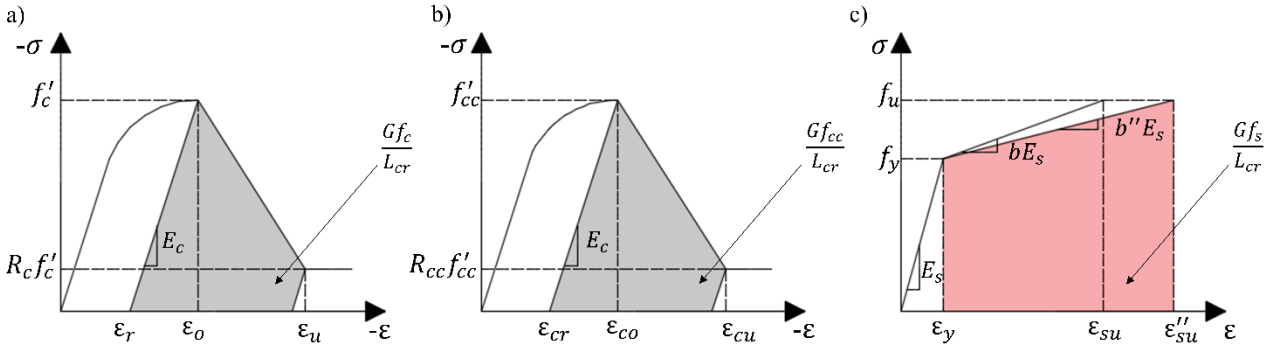

Fig. 1 – Regularization of material stress-strain curves. a) unconfined concrete; b) confined concrete; c) reinforcing steel. Based on [5]

The unconfined and confined concrete crushing energy were calculated using Eq. (5) and Eq. (6), respectively [5], where f_c' is in MPa. The residual stress was taken as 20% of the peak stress [i.e., $R_c = R_{cc} = 0.2$ in Eq. (3) and Eq. (4)] for both unconfined and confined concrete.

$$Gf_c = 2f_c' \tag{5}$$

$$Gf_{cc} = 1.70\, Gf_c \tag{6}$$

Regularization of the reinforcing steel stress-strain relationship was performed using Eq. (7) and Eq. (8) (see Fig. 1c for details), where the gage length, L_{gage} was assumed as 200 mm [5].

$$\varepsilon_{su}'' = \varepsilon_y + \left(\frac{L_{gage}}{L_{cr}}\right)\left(\varepsilon_{su} - \varepsilon_y\right) \tag{7}$$

$$b'' = \frac{f_u - f_y}{E_s\left(\varepsilon_{su}'' - \varepsilon_y\right)} = b\,\frac{\left(\varepsilon_{su} - \varepsilon_y\right)}{\left(\varepsilon_{su}'' - \varepsilon_y\right)} \tag{8}$$

No recommendations for the regularization of concrete and steel materials for the cyclic modeling of RC columns were identified by the authors in the literature. Therefore, Eq. (3) to Eq. (8), which were developed based on experiments of slender RC walls, were also used in this study to evaluate their implications in modeling RC columns.

3. Experimental Database

A database of eight previously tested walls and ten columns, was used to evaluate the numerical models. This database is presented in Table 1, where t and L are the wall thickness and length, respectively, W and H are the column width and height, respectively, H_{eff} is the effective height (defined as the distance between the maximum and zero moment locations), f_c' is the unconfined concrete compressive strength, and f_y is the steel yield stress. All of these specimens presented ultimate failure modes due to concrete crushing (with or without rebar buckling), and therefore, softening post-peak behavior occurred. The specimens were slender (i.e., $M/(Vl) \geq 2$) and had a wide range of material properties and axial load ratios (i.e., $P/(f_c'A_g)$). The last column of Table 1 shows the mean plastic hinge length, $L_{p.mean}$, calculated according to three different available equations for RC walls [15–17] and six different equations for RC columns [18–23].

Table 1 – Experimental wall and column database

RC Walls									
Specimen ID	**Reference**	t **[mm]**	L **[mm]**	H_{eff} **[mm]**	f'_c **[MPa]**	f_y **[MPa]**	$\frac{P}{f'_c A_g}$	$\frac{M}{VL}$	$L_{p,mean}$ **[mm]**
WSH4	[24]	150	2000	4560	40.9	576.0	0.06	2.3	566
WSH6	[24]	150	2000	4520	45.6	576.0	0.11	2.3	539
RW1	[25]	102	1219	3810	31.6	434.5	0.10	3.1	403
WP1	[26]	152	2286	8560	35.8	506.0	0.10	3.7	745
WP2	[26]	152	2286	8560	41.7	506.0	0.08	3.7	757
WP3	[26]	152	2286	8560	42.4	506.0	0.08	3.7	758
WR10	[27]	200	1500	3000	36.2	449.0	0.08	2.0	415
HPCW03	[28]	100	1000	2100	57.2	433.3	0.18	2.1	274
RC Columns									
Specimen ID	**Reference**	W **[mm]**	H **[mm]**	H_{eff} **[mm]**	f'_c **[MPa]**	f_y **[MPa]**	$\frac{P}{f'_c A_g}$	$\frac{M}{VL}$	$L_{p,mean}$ **[mm]**
Unit 1	[29]	400	400	1600	46.5	446.0	0.10	4.0	215
Unit 4	[29]	400	400	1600	40.0	446.0	0.30	4.0	232
Unit 1	[30]	400	400	1600	25.6	474.0	0.20	4.0	243
Unit 6	[30]	550	550	1650	32.0	511.0	0.10	3.0	267
Specimen 9	[31]	305	305	1676	33.3	363.0	0.26	5.5	228
Specimen 11	[31]	305	305	1676	31.0	363.0	0.28	5.5	230
U1	[32]	350	350	1000	43.6	430.0	0.00	2.9	209
U7	[32]	350	350	1000	39.0	437.0	0.13	2.9	217
BG-1	[33]	350	350	1645	34.0	455.6	0.43	4.7	250
BG-4	[33]	350	350	1645	34.0	455.6	0.46	4.7	257

4. Simulation Results

The analysis results obtained using the un-regularized and regularized plastic hinge models are presented in this section. For the regularized models, the mean plastic hinge length ($L_{p,mean}$ in Table 1) was used as the critical integration length, L_{cr} in Eq. (3), Eq. (4), and Eq. (7). The $L_{p,mean}$ was also used for defining the length and weight of the integration points in Eq. (1). The results are evaluated based on the numerical-to-experimental ratios of the effective stiffness (RK_e), maximum strength (RV_{max}), and ultimate displacement ($R\delta_u$). The effective stiffness and maximum strength were calculated from the mean (considering the positive and negative loading directions) backbone curve for each specimen. The effective stiffness was calculated as the slope between the origin and the point on the mean backbone curve corresponding to 70% of the maximum strength. The ultimate displacement was defined as the displacement corresponding to a 20% reduction in lateral load resistance from the maximum strength based on the effective lateral load-displacement curve with P-Δ effects removed as presented in Berry et al. [34] so as to capture material deterioration rather than geometric effects.

The numerical-to-experimental ratios of the evaluation parameters for the wall and column specimens are presented in Table 2. Looking at the mean and standard deviation results for the walls, both the un-regularized and regularized plastic hinge models accurately simulated the effective lateral stiffness and maximum strength. The regularized models also provided accurate predictions of the ultimate displacement, with a mean ratio of 0.94. In comparison, the un-regularized wall models resulted in a highly overestimated

(unconservative) prediction of the ultimate displacement, with a mean ratio of 1.98, and a significantly increased standard deviation. This trend was opposite for the column specimens, where the regularized models resulted in a worse prediction of the ultimate displacement as compared with the un-regularized models, even though there were improvements in the prediction of the effective stiffness and maximum strength.

Overall, the results in Table 2 suggest that: 1) since the concrete stress-strain relationships used in the un-regularized plastic hinge models were obtained mainly from the testing of RC columns [11], they are better in simulating the ultimate displacement of columns than that of walls, 2) the regularized stress-strain relationships significantly improved the accuracy of the ultimate displacement simulations for RC walls, but not for columns, and 3) Eq. (5) and Eq. (6) for the unconfined and confined concrete crushing energy, respectively, are not adequate to simulate the ultimate displacement of RC columns.

The lateral load-displacement behaviors of the RC wall specimens simulated using the regularized plastic hinge model are presented in Fig. 2, while the behaviors of the column specimens simulated using the un-regularized plastic hinge model are presented in Fig. 3. The experimentally measured behaviors of the specimens are depicted in red. These results show that the models were able to capture the complex cyclic behaviors (i.e., strength and stiffness degradation and pinching) of the specimens up to failure reasonably well.

Table 2 – Numerical-to-experimental ratios of evaluation parameters

Specimen ID	**Un-regularized**			**Regularized**		
	RK_e	RV_{max}	$R\delta_u$	RK_e	RV_{max}	$R\delta_u$
RC Walls						
WSH4	1.36	0.91	0.64	1.26	0.97	1.10
WSH6	0.72	0.98	1.73	0.73	0.96	0.86
RW1	1.05	1.06	1.68	1.04	1.07	1.15
WP1	1.10	1.08	2.54	1.11	1.07	0.86
WP2	0.72	1.20	3.28	0.78	1.07	0.80
WP3	0.70	1.15	2.89	0.74	1.06	0.92
WR10	1.09	1.00	2.20	1.13	0.97	1.00
HPCW03	0.94	0.94	0.87	0.94	0.93	0.87
mean	**0.96**	**1.04**	**1.98**	**0.97**	**1.01**	**0.94**
st. dev.	**0.24**	**0.10**	**0.93**	**0.20**	**0.06**	**0.13**
RC Columns						
Unit 1	1.21	0.96	0.67	1.20	0.97	1.05
Unit 4	1.06	0.93	0.61	1.02	0.96	1.16
Unit 1	1.20	0.95	1.08	1.10	1.01	0.63
Unit 6	1.36	0.98	0.96	1.35	1.00	0.74
Specimen 9	1.46	1.03	1.15	1.38	1.05	2.01
Specimen 11	1.21	1.00	1.39	1.16	1.02	2.31
U1	2.02	0.95	0.97	1.20	1.22	1.96
U7	1.61	1.08	0.71	1.61	1.02	0.63
BG-1	0.92	0.82	0.99	0.81	0.90	0.99
BG-4	0.85	0.91	0.97	0.74	1.01	0.70
mean	**1.29**	**0.96**	**0.95**	**1.16**	**1.02**	**1.22**
st. dev.	**0.34**	**0.07**	**0.24**	**0.26**	**0.08**	**0.64**

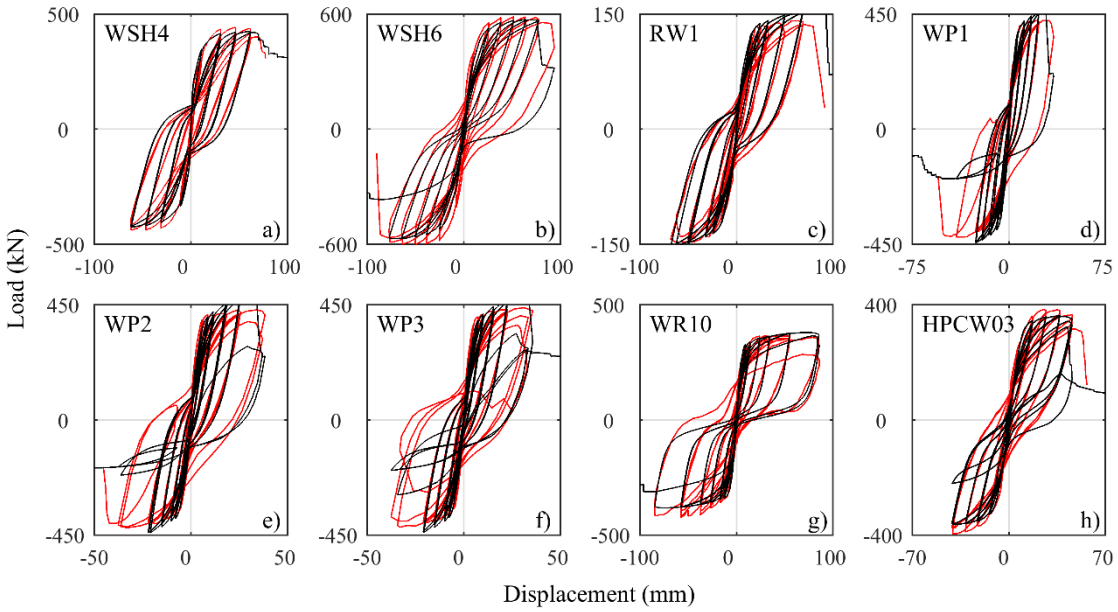

Fig. 2 – Lateral load-displacement behaviors of wall specimens. (Experimental results in red and regularized plastic hinge model results in black)

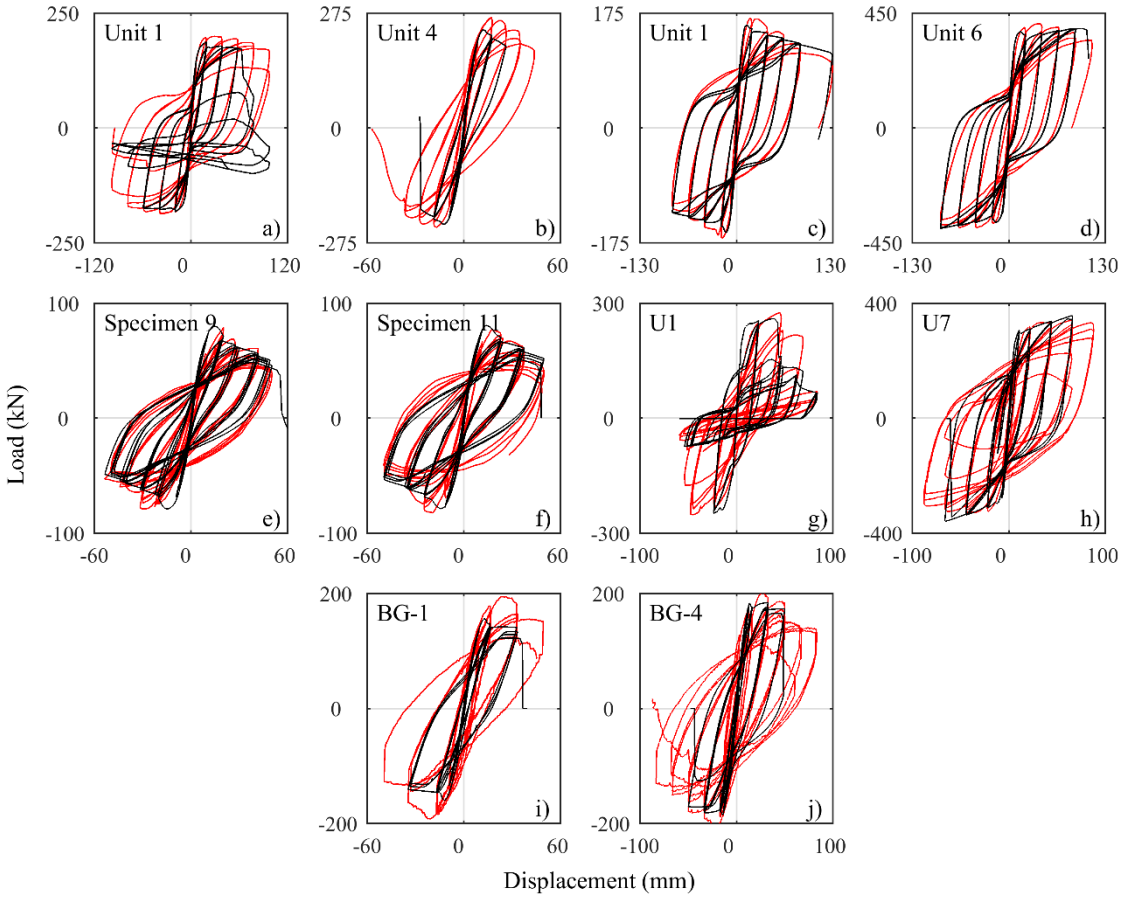

Fig. 3 – Lateral load-displacement behaviors of column specimens. (Experimental results in red and un-regularized plastic hinge model results in black)

5. Sensitivity Analysis

The analysis results in the previous section were obtained using the mean plastic hinge length ($L_{p,mean}$) from Table 1. The sensitivity of the evaluation parameters to the assumed plastic hinge length was also studied because there are many available recommendations for the plastic hinge length of RC walls and columns in the literature. To study the sensitivity of the numerical predictions, parametric analyses were conducted using plastic hinge length values, L_p ranging between 0.75 and 1.25 $L_{p,mean}$. The results showed that the sensitivity of the effective stiffness and maximum strength to the plastic hinge length was generally small for both walls and columns. Contrarily, the ultimate displacement was much more sensitive to L_p, and these results are presented below.

The numerical-to-experimental ultimate displacement ratios ($R\delta_u$) from the un-regularized and regularized plastic hinge models are presented in Fig. 4a,b for the eight wall specimens, and in Fig. 4c,d for the ten column specimens. In general, the ultimate displacement from the un-regularized models (Fig. 4a,c) were very sensitive to the assumed plastic hinge length. The results show an increase of the numerical ultimate displacement as L_p increases, with greater variations when modeling RC walls (Fig. 4a). In comparison, the ultimate displacement from the regularized plastic hinge models (Fig. 4b,d) was much less sensitive to the assumed plastic hinge length. This reduced sensitivity of the regularized models to the assumed plastic hinge length is primarily because of the post-peak stress-strain regularization of the unconfined and confined concrete (Eq. (3) and Eq. (4)) based on the critical integration length (i.e., $L_{cr} = L_p$). Additionally, the results in Fig. 5d further demonstrate the finding that Eq. (5) and Eq. (6) for the unconfined and confined concrete crushing energy, respectively, are not adequate to simulate the ultimate displacement of RC columns. Therefore, improved equations are needed for the concrete crushing energy of RC columns at the onset of failure.

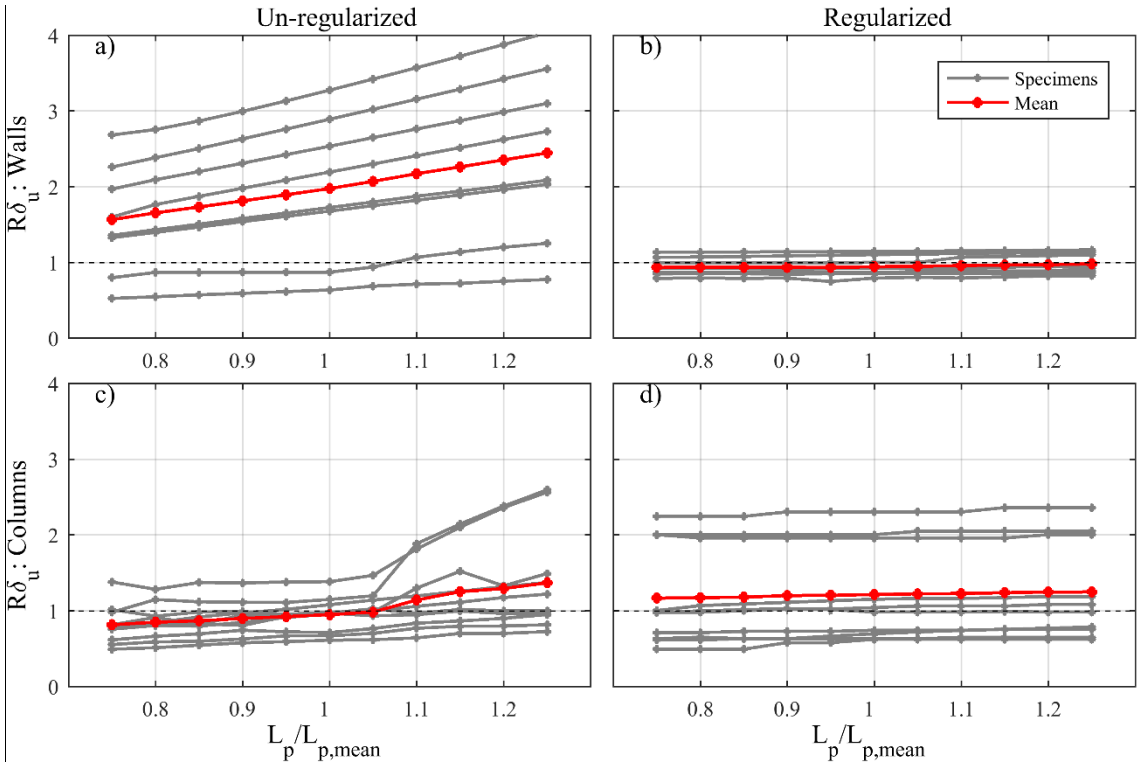

Fig. 4 – Sensitivity of ultimate displacement ratio to assumed plastic hinge length. a) un-regularized wall models; b) regularized wall models; c) un-regularized column models; d) regularized column models

6. Conclusions

This paper presents a numerical investigation comparing the use of traditional and regularized concrete and steel stress-strain relationships in plastic hinge models for the cyclic behavior of RC walls and columns with softening post-peak behavior. The important findings and conclusions from the study are as follows:

1) Un-regularized plastic hinge models with traditional confined concrete stress-strain relationships according to Mander et al. [11] provided adequate predictions of the effective stiffness, maximum strength, and ultimate displacement of RC columns. However, the ultimate displacement was largely overestimated when using these models to simulate RC walls. This difference is attributed to the confined concrete stress-strain relationship used in the un-regularized models, which was calibrated mainly from experiments of RC columns.
2) Regularized plastic hinge models accurately simulated the cyclic behavior or RC walls up to the onset of failure, including the ultimate displacement.
3) Regularized plastic hinge models reduced the accuracy and increased the variability (i.e., larger standard deviation) in the prediction of the ultimate displacement for RC columns, even though the results were slightly improved for the effective stiffness and maximum strength. Thus, improved regularization equations are needed for the concrete crushing energy to accurately simulate the ultimate displacement of RC columns.
4) The ultimate displacement of the un-regularized wall and column models was highly sensitive to the assumed plastic hinge length. This sensitivity was significantly reduced when using regularized models. This is a major advantage of using regularized material stress-strain relationships when modeling the nonlinear behavior of RC walls and columns with softening post-peak behavior.

7. Acknowledgements

The authors would like to acknowledge the financial support of CONICYT Doctorado Nacional 2017 Folio 21171563, CONICYT/FONDAP/15110017 (Research Center for Integrated Disaster Risk Management, CIGIDEN), and CONICYT / FONDECYT 1171062.

8. Copyrights

9. References

[1] Ghannoum WM, Matamoros AB (2014): Nonlinear modeling parameters and acceptance criteria for concrete columns. *ACI Special Publication*, **297**, 1–24.

[2] Haselton CB, Liel AB, Taylor-Lange SC, Deierlein GG (2016): Calibration of model to simulate response of reinforced concrete beam-columns to collapse. *ACI Structural Journal*, **113**, 1141–1152.

[3] Vásquez JA, De la Llera JC, Hube MA (2016): A regularized fiber element model for reinforced concrete shear walls. *Earthqueake Engineering & Structural Dynamics*, **45**, 2063–2083.

[4] Pugh JS, Lowes LN, Lehman DE (2015): Nonlinear line-element modeling of flexural reinforced concrete walls. *Engineering Structures*, **104**, 174–192.

[5] NIST (2017): Recommended modeling parameters and acceptance criteria for nonlinear analysis in support of seismic evaluation, retrofit, and design. NIST GCR 17-917-45. Gaithersburg, MDNational Institute of Standards and Technology.

[6] Scott MH, Fenves GL (2006): Plastic Hinge Integration Methods for Force-Based Beam–Column Elements. *Journal of Structural Engineering*, **132**, 244–252.

[7] Coleman J, Spacone E (2001): Localization issues in force-based frame elements. *Journal of Structural Engineering*, **127**, 1257–1266.

[8] McKenna F, Fenves G, Scott M, Jeremic B (2000): Open system for earthquake engineering simulation (OpenSees). Berkeley, CAPacific Earhquake Engineering Research Center, University of California.

[9] Scott MH, Hamutçuoğlu OM (2008): Numerically consistent regularization of force-based frame elements. *International Journal for Numerical Methods in Engineering*, **76**, 1612–1631.

[10] ACI (2019): Building code requirements for structural concrete (ACI 318-19) and commentary (ACI 318R-19). Farmington Hills, MIAmerican Concrete Institute, Committe 318.

[11] Mander JB, Priestley N, Park R (1988): Theoretical stress-strain model for confined concrete. *ASCE Journal of Structural Engineering*, **114**, 1804–1826.

[12] Menegotto M, Pinto PE (1973): Method of analysis for cyclically loaded R.C. plane frames including changes in geometry and non-elastic behavior of elements under combined normal force and bending. Proceedings, IABSE Symp., Lisbon, Portugal, p. 15–22.

[13] PEER/ATC (2010): Modeling and acceptance criteria for seismic design and analysis of tall buildings, PEER/ATC 72-1. Redwood City, CAPacific Earthquake Engineering Research Center, Applied Technology Council.

[14] Priestley MJN, Seible F, Calvi GM (1996): Seismic design and retrofit of bridges. New YorkJohn Wiley & Sons.

[15] Kazaz İ (2013): Analytical study on plastic hinge length of structural walls. *Journal of Structural Engineering*, **139**, 1938–1950.

[16] Paulay T, Priestley MJN (1993): Stability of ductile structural walls. *ACI Structural Journal*, 385–392.

[17] Bohl A, Adebar P (2011): Plastic hinge length in high-rise concrete shear walls. *ACI Structural Journal*, **108**, 148–157.

[18] Corley WG (1966): Rotational capacity of reinforced concrete beams. *Journal of the Structural Division*, **92**, 121–146.

[19] Mattock AH (1967): Discussion of "Rotational Capacity of Hinging Regions in Reinforced Concrete Beams" by W.G. Corley. *Journal of the Structural Division*, 519–522.

[20] Priestley MJN, Park R (1987): Strength and ductility of concrete bridge columns under seismic loading. *Structural Journal ACI*, **84**, 285–336.

[21] Paulay T, Priestley MJN (1992): Seismic Design of Reinforced Concrete and Masonry Buildings.

[22] Berry MP, Lehman DE, Lowes LN (2008): Lumped-plasticity models for performance simulation of bridge columns. *ACI Structural Journal*, 270–279.

[23] Bae S, Bayrak O (2008): Plastic hinge length of reinforced concrete columns. *ACI Structural Journal*, 290–300.

[24] Dazio A, Beyer K, Bachmann H (2009): Quasi-static cyclic tests and plastic hinge analysis of RC structural walls. *Engineering Structures*, **31**, 1556–1571.

[25] Thomsen J, Wallace J (2004): Displacement-based design of slender reinforced concrete structural walls—experimental verification. *Journal of Structural Engineering*, **130**, 618–630.

[26] Segura CL, Wallace JW (2018): Seismic performance limitations and detailing of slender reinforced concrete walls. *ACI Structural Journal*, **115**, 849–859.

[27] Oh YH, Han SW, Lee LH (2002): Effect of boundary element details on the seismic deformation capacity of structural walls. *Earthquake Engineering and Structural Dynamics*, **31**, 1583–1602.

[28] Deng M, Liang X, Yang K (2008): Experimental study on seismic behavior of high performance concrete shear wall with new strategy of transverse confining stirrups. 14th World Conf. Earthq. Eng., Beijing, China, p. 1–8.

[29] Soesianawati MT (1986): Limited ductility design of reinforced concrete Columns. MEng thesis. University of Canterbury, Christchurch, New Zealand.

[30] Tanaka H (1990): Effect of lateral confining reinforcement on the ductile behaviour of reinforced concrete columns. PhD dissertation. University of Canterbury, Christchurch, New Zealand.

[31] Atalay M, Penzien J (1975): The seismic behavior of critical regions of reinforced concrete components as infuenced by moment, shear and axial force.

[32] Saatcioglu M, Ozcebe G (1989): Response of reinforced concrete columns to simulated seismic loading. *ACI Structural Journal*, **86**, 3–12.

[33] Saatcioglu M, Grira M (1999): Confinement of reinforced concrete columns with welded reinforcement grids. *ACI Structural Journal*, **96**, 29–39.

[34] Berry M, Parrish M, Eberhard M (2004): PEER Structural Performance Database User 's Manual. University of California, Berkeley.

